A New RSS-based Wireless Geolocation Technique Utilizing Joint Voronoi and Factor Graph

Muhammad Reza Kahar Aziz [1,2], Yuto Lim [1], and Tad Matsumoto [1,3]

1 School of Information Science, Japan Advanced Institute of Science and Technology (JAIST), Ishikawa, 923-1292 JAPAN
2 Electrical Engineering Department, Institut Teknologi Sumatera (ITERA), Lampung Selatan, 35365 INDONESIA
3 Centre for Wireless Communications, University of Oulu, Oulu, 90014 FINLAND
Email: {reza.kahar, ylim, matumoto}@jaist.ac.jp

***Abstract* — This paper proposes a new joint received signal strength (RSS)-based Voronoi and factor graph (RVFG) wireless geolocation technique. The RSS-based Voronoi (RV) technique is used to provide the initial position for the RSS-based factor graph (RFG) technique. The initial point obtained by the RV is used to select the appropriate four monitoring spots which are covering the target for the RFG. We also modify the RV so that it can be performed in the fusion center. The proposed technique is tested in outdoor environment where only path-loss is taken into account. The performance of the proposed technique in term of the root mean square (RMSE) is compared to that of the conventional RV only technique. The results show that the accuracy of the proposed technique outperforms the conventional RV technique. The material in this paper was presented in part at Asia Modelling Symposium, Kuala Lumpur, September 2015 [1].**

Keywords – factor graph, monitoring spots, Voronoi diagram, wireless geolocation, RSS

I. INTRODUCTION

Wireless geolocation achieving high accuracy is needed to provide location-related services in communications. The location-related services play crucial roles in reliable and safety society such as Emergency-911 (E-911), location based billing service, intelligent transportation systems, car navigation, elderly people tracking, and accurate harvest control in agriculture [2]–[4]. This research field has gained considerable attention since the past two decades.

In 2013, the first geolocation technique utilizing turbo (iterative) processing to perform location detection by using factor graph (FG) was introduced in [5], which was a few years after the mathematical framework of the FG was first introduced in [6]. It should be noted that the FG-based geolocation is a technological basis for identifying the location where radio waves are transmitted. Other geolocation techniques, e.g., Gauss-Newton (GN), Nonlinear Least Square (NLSS), Method of Moments (MOM), require likelihood function calculation based on empirical covariance matrix, which imposes high computational complexity for solving non-linear problems [7]–[9]. The FG-based techniques have several benefits because the FG-based techniques require only solving linear problem, which can efficiently utilize the stochastic information as discussed in [8]–[11].

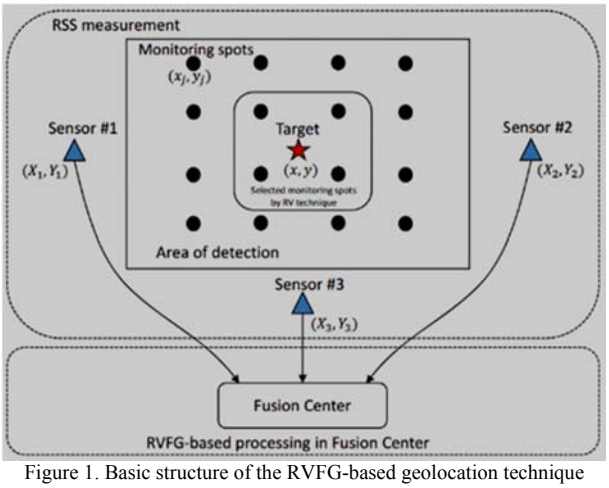

Figure 1. Basic structure of the RVFG-based geolocation technique describing sensors, target, monitoring spots, and fusion center.

The FG uses sum-product algorithm via message passing to compute the marginal function derived from global function, and hence the FG effectively coordinates all stochastic information to obtain high accuracy in geolocation. This global function, in the FG, factors to several simple local function that makes the complexity of the FG algorithm low. This complexity reduction is achieved by the fact that only mean and variance are used as messages in the FG due to the Gaussianity assumption of the measurement error [6], [8]–[11].

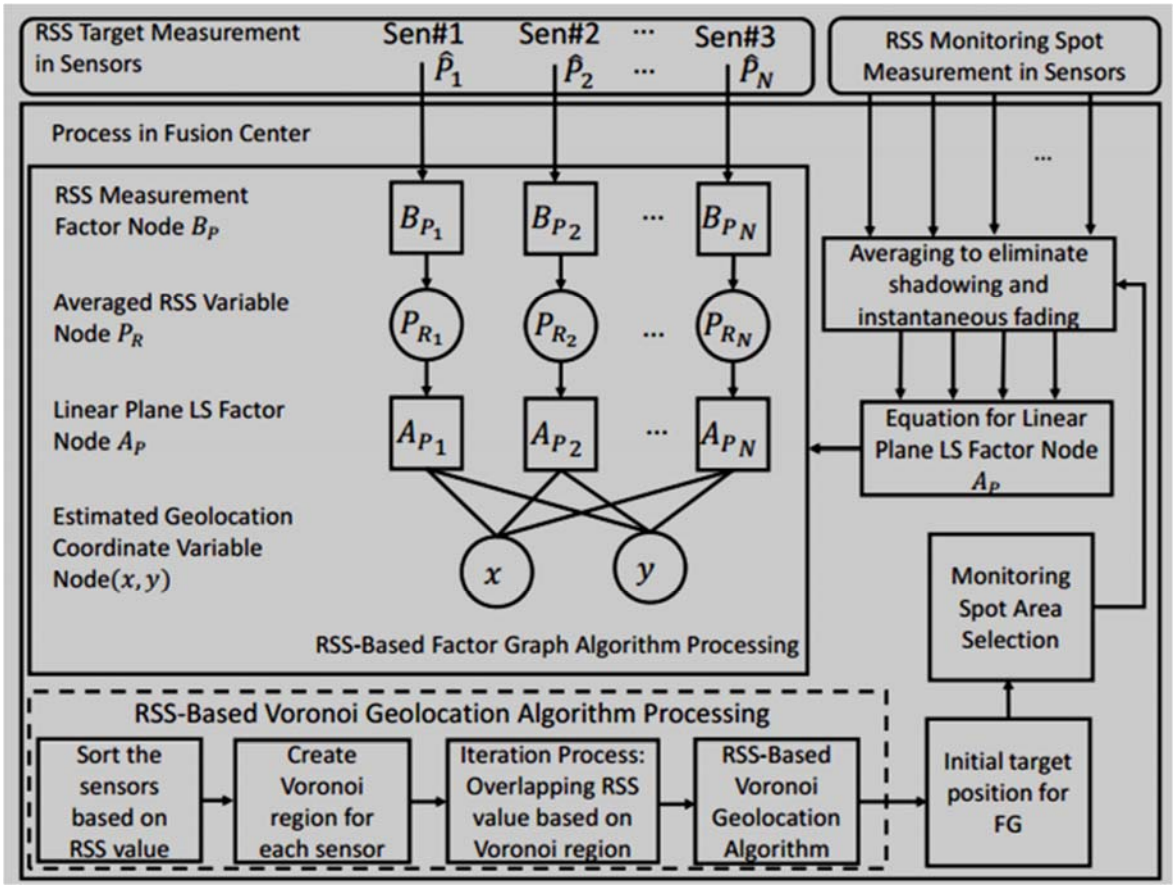

Figure 2. The proposed RVFG for Geolocation Technique.

This paper proposes new scheme to select four appropriate monitoring spots covering the target.

Notes:

1. We use the terminology of monitoring spot instead of training point mentioned in [11] for monitoring radio system.
2. We use the terminology of RSS instead of RSS indicator (RSSI) because we use dB as the unit for the measurement result.
3. RADAR stands for a radio-frequency (RF) based system for locating and tracking users inside buildings [12].
4. We use the shorter term in the rest part in this paper, e.g., ”the RV” instead of ”the RV geolocation technique” for simplicity.

The selected monitoring spots are used for received signal strength (RSS) -based FG (RFG) geolocation technique as shown in Figs. 1 and 2 (See large figure 2 at the end of the paper). This RFG technique, which is introduced by [11], utilizes pattern-recognition technique, i.e., RADAR, to find four appropriate monitoring spots covering the target. However, the process to select the monitoring spots is not explained in detail in [11]. The technique proposed in this paper, socalled RSS-based Voronoi FG (RVFG) technique, utilizes the initial point given by conventional RSS-based Voronoi (RV) geolocation technique [13] to select the monitoring spots for the RFG.

A. Related Work

The RFG in [11] detects the target position in indoor areas of wireless networks. They assume that the environment is solely suffering from shadowing variations. The state of the art of their technique lies in how close the linear plane can be made by the RSS information from the monitoring spots to approximate the real RSS profile. The least square (LS) is used to obtain the linear plane equation for the profile approximation.

In [14], we have investigated the RFG in outdoor environments, where solely path-loss is taken into account. The shadowing and instantaneous attenuation components are eliminated by assuming a long range enough averaging. We also found that the accuracy of the RFG depends on the width size of monitoring spot area covering the target. Furthermore, if the target is surrounded by four monitoring spots, adding more monitoring spots does not increase the accuracy.

The algorithm of RV [13] is briefly described in [15]. According to the technique shown in [13], the target

receives the RSS information from the beacons, hence the target processes the RSS information to detect its own position estimate. The position estimate is obtained by accumulating the measured RSS belonging to each Voronoi region. After that, the algorithm was improved in [15] by employing the triangle algorithm between two sensors and the target to obtain the straight line. The several crossing points made by several straight lines are close to the target position. The measured RSS value is included to the expectation of the crossing points as weighting factor in calculating the position estimate. In the RV, high accuracy is achieved with the large number of sensors.

B. Contributions

The main contribution of this paper is that we propose a joint use of the conventional RV and RFG techniques, where RV is used to select the appropriate four monitoring spots of RFG covering the target. The RV also provides the initial value for iteration in the RFG algorithm. The RFG itself improves the accuracy of the RV. The main objectives of this paper are as follows: 1) We modify the conventional RV algorithm in [13] with the opposite way, i.e., the sensors measure the RSS of the target and then forward it to fusion centre, where the RV algorithm is performed in fusion centre. 2) We combine the modified RV with the RFG to improve the accuracy, where RV is used to select four monitoring spots, which are covering the target, for RFG. 3) We compare the performance of the proposed technique with sensor numbers and signal to noise power ratio (SNR) as parameters. 4) The outdoor environment is assumed where long enough averaging range is performed to eliminate the shadowing and instantaneous attenuation, hence the only path-loss still remains as in [14].

II. SYSTEM MODEL

The target position to be estimated is at x=(x,y)^T, where T indicates the transposition of the argument vector. Multiple N sensors perform measurement of RSS signal sent from both the target and monitoring spots, where the position is indicated by X=(X_(i,) Y_i)^T, with i=1,2,...,N being the sensor index. Multiple M monitoring spots send training signal to the sensors, where the position is indicated by Y=(x_j,y_j)^T, with j=1,2,...,M being the monitoring spot index.

As mentioned above, only path-loss component remains in the RSS samples of the signal sent from the target as well as from the monitoring spots in the training process. This is due to the free space loss assumption. In addition, when the free space loss condition is unavailable, the condition that the only path-loss component remains can also be achieved by performing measurement around the initial sensor position (X_i,Y_i),i,i=1,2,...,N. The areas for the averaging by each sensor are large enough to eliminate the shadowing components in the RSS samples. The profile of RSS at sensor position (900,-420) m is shown in Fig. 3, where the path-loss exponent model is used as

$$P_i(d_i) = 20\log\left(\frac{4\pi d_0 f_c}{c}\right) + 10n\log\left(\frac{d_i}{d_o}\right), \quad (1)$$

where d_0 denotes reference distance, f_c denotes carrier frequency, and n denotes path-loss exponent. d_i denotes Euclidean distance from target or monitoring spot to the i-th sensor [14], [16], as

$$d_i = \sqrt{(X_i - x)^2 + (Y_i - y)^2}. \quad (2)$$

We use P_i instead of $P_i(d_i)$ in the rest of this paper for simplicity, where P_i is in unit of dB.

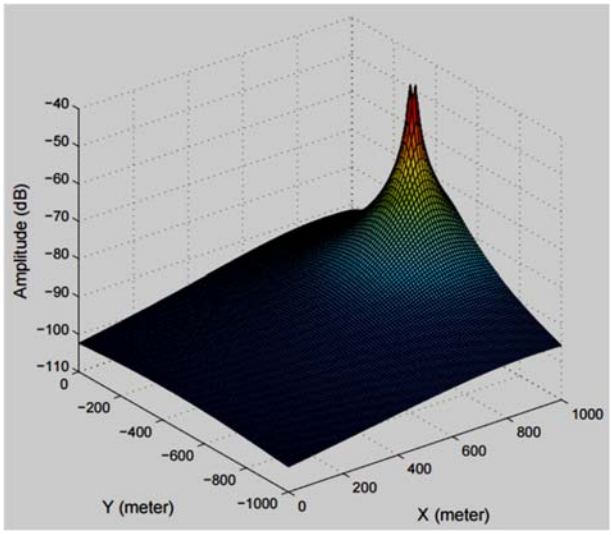

Figure 3. RSS profile of path-loss model with sensor position at $(900, -420)$ m, $n = 3$ for urban area, $f_c = 1$ GHz, and $d_0 = 100$ m.

We assume that the RSS samples are corrupted by zero mean Gaussian noise as in [8], [10], [11]. This assumption is reasonable because of the effect of accumulation of many independent factors, including temporal spread due to multipath, and spatial spread. In the sensor, the measured RSS sample $\hat{P}_{w,i}$ with path-loss component only is corrupted by Gaussian noise as:

$$\hat{P}_{w,i} = P_{w,i} + n_{w,i}, \quad (3)$$

where $P_{w,i}$ denotes the true value of RSS target sample in unit of watt. In our computer simulation, we obtain $P_{w,i}$ from (1), where $P_{w,i} = 10^{P_i/10}$. The measurement error is

denoted by $n_{w,i}$ as zero-mean Gaussian noise.Thus, the RSS sample $\hat{P}_{w,i}$ follows a Normal distribution $\mathcal{N}\left(P_{w,i}, \sigma^2_{P_{w,i}}\right)$ with a probability density function $p(\hat{P}_{w,i})$

$$1. \quad p(\hat{P}_{w,i}) = \frac{1}{\sqrt{2\pi}\sigma_{P_{w,i}}} \exp\left(\frac{-(\hat{P}_{w,i}-P_{w,i})^2}{2\sigma^2_{P_{w,i}}}\right). \qquad (4)$$

However, the RSS samples used in the RV, RFG, and RVFG are in the units of dB, for which we need a validation of Gaussian approximation when converting the unit watt to dB. A relatively accurate approximation for this purpose can be found in [11], which this paper also follows.

III. RVFG GEOLOCATION TECHNIQUE A.

RV Geolocation Technique The RV technique is used to select four monitoring spots for RFG algorithm as shown in Fig. 2. The following process of RV algorithm is modified from [15] so that it can be performed in the fusion center: 1) Create the Voronoi diagram based on sensors position. 2) Sort the sensors based on RSS value, where sensor with the highest RSS value is in the first position. 3) Add plots having the highest RSS value to the first Voronoi region. 4) Remove the first sensor from the system. 5) Re-create the Voronoi region based on the rest of sensors, where the second sensor works as the new first sensor. 6) Add the plots having the second largest RSS value to the new Voronoi region of the next first sensor. 7) Repeat the processes of 3) to 6) until the calculation of the last sensor completed. 8) Obtain the target position by calculating the expectation of the coordinate positions with the highest accumulated RSS value.

Fig. 4 shows the Voronoi diagram with 23 sensors. One of the Voronoi region with the highest measured RSS value is assigned with its measured RSS value. After that, since the sensor having the highest measured RSS value is removed, there remain only 22 sensors. The Voronoi region of the sensor, with highest measured RSS value among 22 sensors, is added with its own RSS value. Hence, there is accumulation and overlapping between the first Vornoi region and the second Voronoi region. When all sensors are removed, we have the overlapping accumulation of RSS value from 23 sensors, as shown in Fig. 5. It is found that the region having the highest accumulated RSS of target measured by 23 sensors are close to the true target position, which is at (468,-838) m. The position estimate is obtained from the average of the coordinates having the highest accumulated RSS, which is at (477,-840) m.

The computational complexity of RSS value accumulation performed for the overlapped Voronoi region in the RV depends on the resolution of the region. This means that higher resolution requires heavier computation, for example, the resolution with grid 10 m2 has lower complexity compare to higher resolution with grid 1 m2. We tested the computation time of the RVFG, FRG, and RV with parameter setting described in Table II. The computation time of the RVFG, RFG, and RV is shown in Table. I. The RFG which is using only 3 sensors has much lower computation time over the RVFG and RV. One of the schemes that can be used to solve the complexity issue is by using pre-computing for the RV before using the technique for geolocation. The result of pre-computing of RSS is simply used as a look-up table. However, pre-computing of the RV is not discussed in detail in this paper because we leave it as a future work.

TABLE I. THE COMPUTATION TIME OF RFVF, RFG, AND RV TECHNIQUES.

Sensor Number	Time Processing (second)		
	RVFG	RFG	RV
3	1.2036	0.0086	1.195
23	25.9462	--	25.93755

B. RFG Geolocation Technique

The RFG presented in this sub-section is based on the technique introduced in [11]. We modify the environment from indoor area suffering from shadowing variation [11] to the outdoor area experiencing from path-loss only [14]. Before performing the RV and RFG in the RVFG algorithm, the sensors measure the RSS samples using training signals sent by monitoring spots. The measurement is performed in a long range enough around the sensors for averaging so that the measurement data contains only path-loss information.

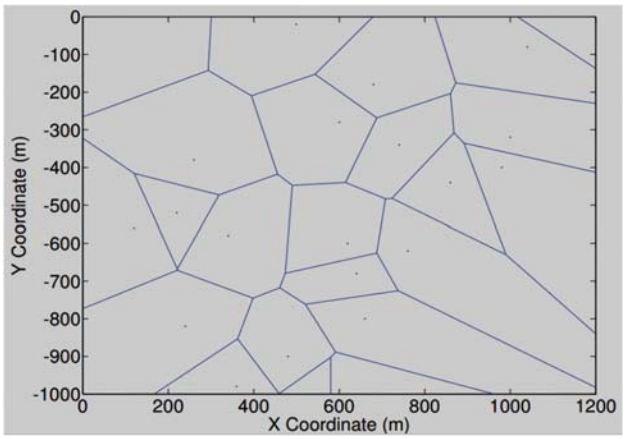

Figure 4. The Voronoi diagram with 23 sensors in 1, 000 × 1, 000 m2.

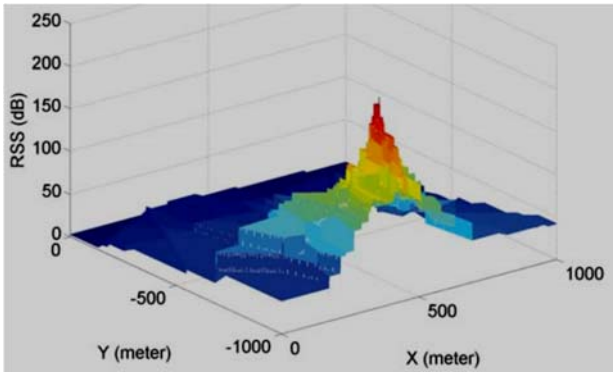

Figure 5. The RSS of target accumulation by the RV algorithm with 23 sensors, where the target is at (468, −838) m.

The RSS samples of training signal sent from monitoring spot are also measured by the sensor in long duration to obtain sufficient number of the RSS samples. Hence, the averaging of those RSS samples results the RSS value of monitoring spots which is free from measurement error [11]. It should be noted that the RSS samples of the target still contain measurement error with containing only path-loss component. All measured RSS samples by the sensor are sent to the fusion center, where the RVFG geolocation algorithm is performed. The error-free measured RSS samples of the training signals are used for establishing the equation at *linear plane LS factor nodes* A_p, where RSS samples of the target is converted into the target position.

The linear plane equation used to convert the messages of RSS from target to the coordinate is derived in [11], as:

$$a_{x_i} \cdot x_j + a_{yi} \cdot y_j + a_{pi} \cdot P_{m_{i,j}} = c, \tag{5}$$

where for the i-th sensor, a_{x_i}, a_{y_i}, and a_{p_i} are the coefficients of x, y, and P_i variables of linear plane (8), respectively, to be obtained by solving the LS equation (7), (x_j, y_j) is the position of the j-th monitoring spot, $P_{m_{i,j}}$ is the RSS of the j-th the monitoring spot, obtained from the training sequence, and c is a constant which is set as 1. The matrix equation from (4) is expressed as below

$$\mathbf{B} \cdot \mathbf{a} = \mathbf{c}, \tag{6}$$

where $\mathbf{B}$ is matrix of x_j, y_j, and $P_{m_{i,j}}$ as $\mathbf{a}$ is vector of a_{x_i}, a_{y_i}, and a_{p_i}, and $\mathbf{c}$ is constant vector, as

$$\mathbf{B} = \begin{bmatrix} x_1 & y_1 & p_{m_{i,1}} \\ x_2 & y_2 & p_{m_{i,2}} \\ x_3 & y_3 & p_{m_{i,3}} \\ x_4 & y_4 & p_{m_{i,4}} \end{bmatrix}, \mathbf{a} = \begin{bmatrix} a_{x_i} \\ a_{y_i} \\ a_{p_i} \end{bmatrix}, \mathbf{c} = \begin{bmatrix} 1 \\ 1 \\ 1 \\ 1 \end{bmatrix}. \tag{7}$$

The coefficient of the variables are obtained by employing the least square (LS) solution to (5), as

$$\mathbf{a} = (\mathbf{B}^T \cdot \mathbf{B})^{-1} \cdot \mathbf{B}^T \cdot \mathbf{c}, \tag{8}$$

where $(\cdot)^{-1}$ is the inverse matrix of its argument, and $(\cdot)^T$ is the matrix transpose. The coefficients in a from (7) are used for the final linear plane equation to convert target RSS to the target coordinate (x,y) as expressed below

$$a_{x_i} \cdot x + a_{y_i} \cdot y + a_{p_i} \cdot P_i = c, \tag{9}$$

where P_i is the RSS of target. In the RFG algorithm, P_i contains the information of mean and variance of k RSS samples from the target. The node A_p uses (8) to convert the target RSS message to the target position in the coordinate. The summary of formulas for updating the mean and variance at each node of the RFG can be found from Table I in [11], where the massage flow in the RFG algorithm is described below.

Now, since the equations to be calculated in the node A_P is established, we can start the FG algorithm. The first step in the FG algorithm is conducted in *RSS measurement factor node* B_p to feed the mean $m_{B_{p_i}} \rightarrow P_{R_i}$ and variance $\sigma^2_{B_{p_i}} \rightarrow P_{R_i}$massages extracted from k RSS samples of the target, corrupted by zero-mean Gaussian measurement error, to the averaged RSS variable node P_R, as shown in Fig. 2. The node P_R forwards the RSS messages of the target in the form of mean and variance, obtained from the node B_P to the node A_P as:

$$m_{P_{R_i}} \rightarrow A_{P_i} = m_{B_{P_i}} \rightarrow P_{R_i}, \tag{10}$$

$$\sigma^2_{P_{R_i}} \rightarrow A_{P_i} = \sigma^2_{B_{P_i}} \rightarrow P_{R_i}. \tag{11}$$

The messages of the mean and variance of RSS samples as well as the x and y coordinate are exchanged iteratively between the nodes A_P and the estimated geolocation coordinate variable node (x,y) in FG as shown in Fig. 2. In the node A_P, the messages of mean and variance of RSS are converted to the target (x,y) coordinate, as:

$$m_{A_{P_i} \rightarrow x} = \alpha_{x_i} + \beta_{x_i} \cdot m_{y \rightarrow A_{P_i}} + \gamma_{x_i} \cdot m_{P_{R_i} \rightarrow A_{P_i}}, \tag{12}$$

$$m_{A_{P_i} \rightarrow y} = \alpha_{y_i} + \beta_{y_i} \cdot m_{x \rightarrow A_{P_i}} + \gamma_{y_i} \cdot m_{P_{R_i} \rightarrow A_{P_i}}, \tag{13}$$

$$\sigma^2_{A_{P_i} \rightarrow x} = \beta^2_{x_i} \cdot \sigma^2_{y \rightarrow A_{P_i}} + \gamma^2_{x_i} \cdot \sigma^2_{P_{R_i} \rightarrow A_{P_i}}, \tag{14}$$

$$\sigma^2_{A_{P_i} \rightarrow y} = \beta^2_{y_i} \cdot \sigma^2_{x \rightarrow A_{P_i}} + \gamma^2_{y_i} \cdot \sigma^2_{P_{R_i} \rightarrow A_{P_i}}, \tag{15}$$

where

$$\alpha_{x_i} = \frac{c}{a_{x_i}}, y_i = \frac{c}{a_{y_i}}, \beta_{x_i} = -\frac{a_{y_i}}{a_{x_i}}, \beta_{y_i} = -\frac{a_{x_i}}{a_{y_i}}, \gamma_{x_i} = -\frac{a_{P_i}}{a_{x_i}}, \gamma_{y_i} = -\frac{a_{P_i}}{a_{y_i}}. \tag{16}$$

During the iteration, the node (x,y) forwards the messages, obtained as the result of the sum-product algorithm performed in the node (x,y), back to the node A_P [6], [11], as

$$\prod_{h=1,h=i}^{N} \mathcal{N}(x, m_h, \sigma_h^2) \propto \mathcal{N}\left(x, m_{\Lambda_{x_i}}, \sigma_{\Lambda_{x_i}}^2\right), \quad (17)$$

where the fact that product of independent identically distributed (i.i.d.) Gaussian variable is also Gaussian-distributed is used with h,h =1 ,2,...,N, being the sensor index. As shown in [6], the sum-product algorithm has closed form, as

$$\frac{1}{\sigma_{x\to A_{P_i}}^2} = \sum_{h=1,h\neq i}^{N} \frac{1}{\sigma_{A_{P_h}\to x}^2}, \quad (18)$$

$$\frac{1}{\sigma_{y\to A_{P_i}}^2} = \sum_{h=1,h\neq i}^{N} \frac{1}{\sigma_{A_{P_h}\to y}^2}, \quad (19)$$

$$m_{x\to A_{P_i}} = \sigma_{x\to A_{P_i}}^2 \sum_{h=1,h\neq i}^{N} \frac{m_{A_{P_h}\to x}}{\sigma_{A_{P_h}\to x}^2}, \quad (20)$$

$$m_{y\to A_{P_i}} = \sigma_{y\to A_{P_i}}^2 \sum_{h=1,h\neq i}^{N} \frac{m_{A_{P_h}\to y}}{\sigma_{A_{P_h}\to y}^2}. \quad (21)$$

When the iteration converges, the node (x,y) combines all incoming messages from the node A_P, as

$$\frac{1}{\sigma_x^2} = \sum_{i=1}^{N} \frac{1}{\sigma_{A_{P_i}\to x}^2}, \quad (22)$$

$$\frac{1}{\sigma_y^2} = \sum_{i=1}^{N} \frac{1}{\sigma_{A_{P_h}\to y}^2}, \quad (23)$$

$$m_x = \sigma_x^2 \sum_{i=1}^{N} \frac{m_{A_{P_i}\to x}}{\sigma_{A_{P_i}\to x}^2}, \quad (24)$$

$$m_y = \sigma_y^2 \sum_{i=1}^{N} \frac{m_{A_{P_i}\to y}}{\sigma_{A_{P_i}\to y}^2}, \quad (25)$$

where the mean value (m_x, m_y) indicates the final estimate of the target position.

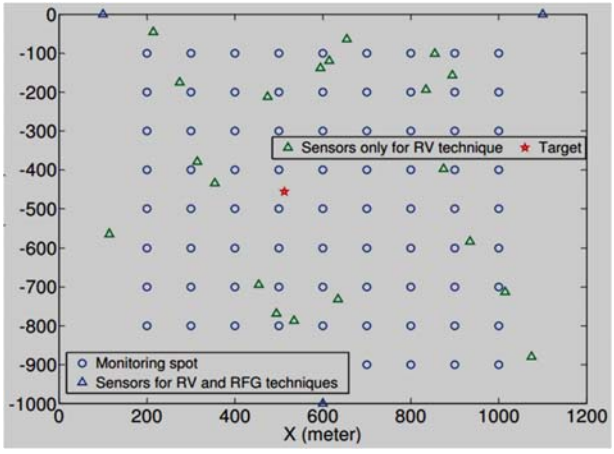

Figure 6. The simulation setup describing monitoring spots with grid 100 × 100 m^2, 23 sensors, 1 targets in total outdoor area of 1,000 × 1,000 m^2.

Since the FG-based geolocation was introduced more than 10 years ago by [5], various derivative algorithms using different wireless parameters have been proposed, such as TOA-based FG [10], TDOA-based Hyperbolic FG [8], and RSS-based FG [11]. However, the proof of the algorithm convergence in fully mathematical way has not yet been given. This is because the difficulty in the analysis due to the cycles appearing inside the FG as mentioned in [8]. Despite the controversy of the convergence analysis, the functions in the FG-based techniques in many cases well behave as mentioned in [10]. Hence, it can be concluded that the FG techniques are near-optimum solution as mentioned also in [8], [11] for wireless geolocation problems.

C. RVFG Geolocation Technique

The RVFG technique is a joint use of the RV and RFG techniques. The RV is used to provide the RFG algorithm with the initial point of the target and proper monitoring spots surrounding the target. The pseudo code of the proposed RVFG technique can be found at Algorithm 1.

IV. SIMULATION RESULTS

A series of computer simulations was conducted to verify the performance of the proposed technique. The simulation round consists of 100 trials, each having one target randomly chosen from the area of 800 × 800 m2. Three sensors used by RFG technique are set at fixed the positions of (100,0),(100,-1000),(600,-1000) m in (X,-Y) coordinate as shown in Fig. 6. Each trial has also additional numbers of sensors, i.e, 0 to 20 sensors, randomly chosen from the area of 1,000×1,000 m2, where all of the sensors in total are used by RV.

The monitoring spot positions are set in a square area of 1,000 × 1,000 m2 with grid step in 100 × 100 m2 as suggested in [14]. The RV is used to select one cell having four monitoring spots, covering the target position. The results are followed by the RFG technique to obtain the accurate position estimate of the target by using the selected four monitoring spots and initial value provided by RV technique. The RFG technique also uses only three sensors which are set at the fixed positions.

The RSS values of target measured in sensors are made by path-loss exponent model because of the long enough averaging range assumption to eliminate the shadowing and instantaneous attenuation as in [14]. We set the path-loss exponent n =3, reference distance d_0 = 100 m, and frequency carrier f =1 GHz.

The following parameters were used to evaluate the accuracy of the proposed technique: a) 30 times of iterations for each trial, b) 100 samples, c) 3 to 23 sensors. The values of the measurement error is in SNR, i.e., 0 to 30 dB. We assume that the measurements are corrupted by the measurement error having the same variance in each sensor

for simplicity. The summary of computer simulation setting can be found in Table. II.

Algorithm 1 : RVFG

---

procedure RV
  Input: RSS samples and sensors position
  calculate mean and variance k RSS samples
  sort and make indexing the sensors
  calculate meshgrid (xi, yi)
  for $ii = 1$ until N sensors do
    calculate $d_i(xi, yi)$ to each grid (2)
  end for
  for $ii = 1$ until N sensors do
    P_{RV} = maximum of $P_i \in N + 1 - ii$
    for all $d_i(xi, yi$ **do**
      if $d_i(xi, yi)$ minimum to other sensors **then**
        $P(xi, yi) = P(xi, yi) + P_{RV}$
      end if
    end for
    remove the selected sensors, $i \in N - ii$
  end for
  select the grid (xi, yi) with maximum $P(xi, yi)$
  Output: inital target of RFG, $(x^0, y^0) = E[(xi, yi)]$
end procedure
procedure SELECT MONITORING SPOTS
  Input: $(\Delta x_j, \Delta y_j) = (x^0 - x_j, y^0 - y_j)$
  (x_r, y_r) = sort (x_j, y_j) based on $(\Delta x_j, \Delta y_j)$
  for $si = 1$ until M monitoring spots do
    if $si = 1$ then
      $x_{s_1} = x_r(1)$, $y_{s_1} = y_r(1)$
    else
      if $x_r(si) = x_r(1)$ **then** do nothing
      else
        $x_{s_2} = x_r(si)$
        break
      end if
      repeat: line 29 – 33 for y coordinate
    end if
  end for
  Output: selected monitoring spots $(x_{s_1}, y_{s_1}), (x_{s_2}, y_{s_1}), (x_{s_1}, y_{s_2}), (x_{s_2}, y_{s_2})$
end procedure
procedure RFG
  Input: Sensors position, selected monitoring spots, and RSS samples
  calculate the coefficients (8), (15)
  for $ti = 1$ until T iteration **do**
    calculate $\sigma^2_{A_{P_1} \to x}, m_{A_{P_1} \to x}$ (13), (11)
    calculate $\sigma^2_{x \to A_{P_1}}, m_{x \to A_{P_1}}$ (17), (19)
    calculate $\sigma^2_{A_{P_1} \to y}, m_{A_{P_1} \to y}$ (14), (12)
    calculate $\sigma^2_{y \to AP_1}, m_{y \to A_{P_1}}$ (18), (20)
  end for
  calculate σ^2_x, σ^2_y (21), (22)
  Output: target coordinate, (m_x, m_y) (23), (24)
end procedure

TABLE II. SIMULATION PARAMETERS.

Parameters	Values
N Sensors	3, 13, and 23
K Samples	100
Trial	100
(X, Y) fixed in meter	$(100,0), (100,-1000), (600,-1000)$ Other sensor positions are random
n path-loss exponent	3
f GHz	1
d_0 meter	100
Iteration times	30
Target area in m^2	800×800
Sensor area in m^2	1000×1000
SNR in dB	0 to 30

Figs. 7 and 8 show the trajectory of the proposed technique with 23 sensors. The initial value provided by RV is close to the target position at (498,-463) m because of many sensors involved, hence the accumulation of the measured RSS value concentrated at averaged coordinate at (500,-464) m, near to the target position. The trajectory of proposed technique is compared to the trajectory of the idealistic of RFG curve where correct monitoring spots are always selected. The initial value is set at (0,0) m. The RV with small number of sensors selects the wrong monitoring spots area as shown in Fig. 9, with the sensor numbers of three. Therefore, the proposed technique can not reach close to the true target position.

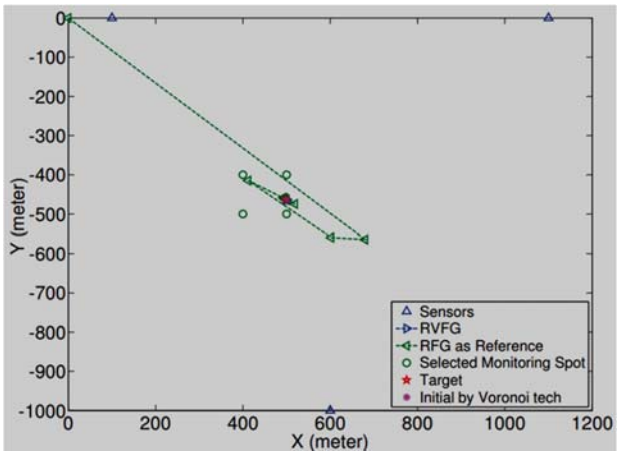

Figure 7. The trajectory of the RVFG technique with 23 sensors (in this figure only shown 3 sensors used by FG-based for simplicity in analysis) and target at $(498, -463)$ m.

Figs. 10 and 11 show the accuracy of the proposed technique in term of RMSE with sensor numbers as a parameter. It is shown that the accuracy with 23 sensors is better than that with 3 and 10 sensors because the larger the number of sensor the higher the accuracy of the initial value given by the RV for selecting the appropriate four monitoring spots for the FG technique. It can be seen that when the iteration converges, the RMSE curve of the RVFG with 23 sensors is asymptotically equal to the idealistic RFG, while the curves with 3 and 13 sensors are asymptotically worse to the idealistic RFG. Hence, the RVFG having the initial point given by the RV with 23 sensors and above is sufficient, in most cases, to correctly select the four appropriate monitoring spots. Fig. 10 shows that the RVFG is faster to converge, requiring around 5 iterations, while the RFG alone requires around 10 iterations to converge. This is because the FG algorithm with RVFG has initial value much closer to the target rather than the RFG alone which is set at (0,0) m.

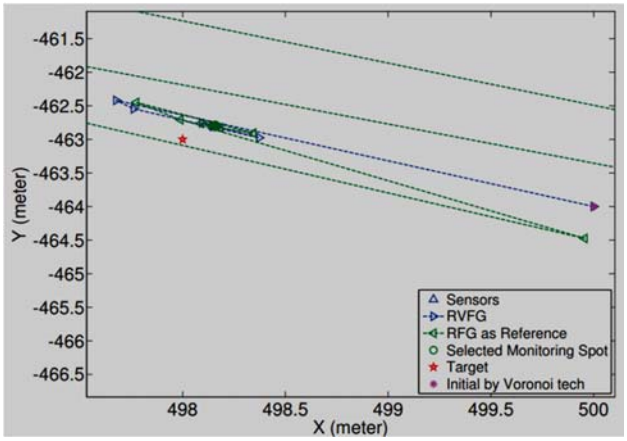

Figure 8. Zoom of the trajectory of the RVFG technique with 23 sensors (in this figure only shown 3 sensors used by FG-based for simplicity in analysis) and target at $(498, -463)$ m.

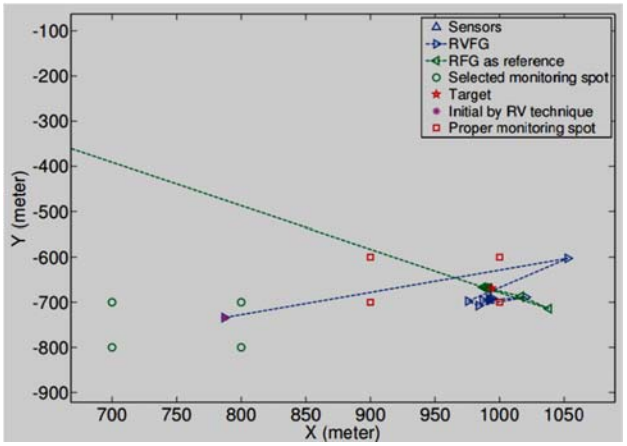

Figure 9. Zoom of the trajectory of the RVFG technique with 3 sensors (the sensors are now shown because of the zoom of the figure) and target at $(994, -669)$ m.

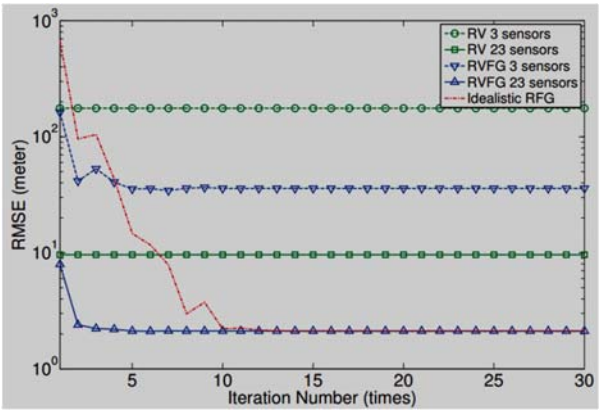

Figure 10. RMSE vs. iteration times with 3 sensors and 23 sensors over 100 trials, and SNR of 15 dB

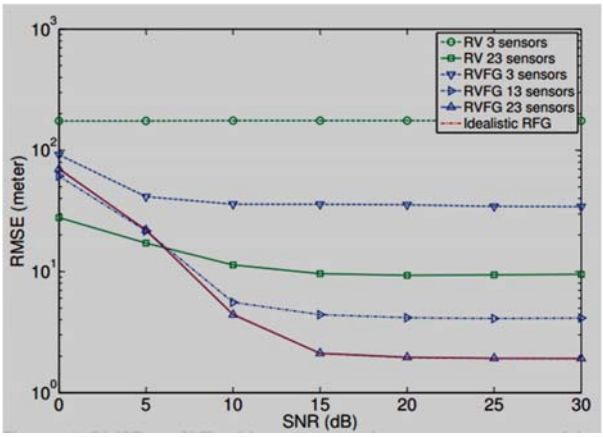

Figure 11. RMSE vs. SNR with 3 sensors and 23 sensors over 100 trials, and 30 times of iteration.

The proposed technique outperforms the conventional RV for SNR more than 7 dB with 23 sensors. For example, the improvement in estimation accuracy with the proposed technique over the conventional RV is approximately 7.5 m at the SNR of 15 dB. Obviously, the tendency of the RMSE curve decreases with the increased SNR values as shown in Fig. 11.

V. CONCLUSION

We have proposed a new wireless geolocation technique using joint RSS-based Voronoi and factor graph (RVFG). The RV geolocation is used to select the area of monitoring spots for RFG geolocation algorithm, as well as to provide its inital value. The simulation results confirmed that our proposed technique provides higher accuracy compared to the conventional RV technique. This technique is suitable for outdoor environment in the future location based applications. Reducing the complexity due to the RV technique by using pre-computing processing is left as a future study. Fully mathematical analysis of the convergence property of the FG techniques is also left as a future work.

REFERENCES

[1] M. R. K. Aziz, Y. Lim, and T. Matsumoto, "A new wireless geolocation technique using joint RSS-based Voronoi and factor graph," 9th Asia Modelling Symposium (AMS) 2015, pp. 132–136, Sep 2015.

[2] J. James J. Caffery and G. L. Stuber, "Overview of radiolocation in CDMA cellular systems," IEEE Communications Magazine, vol. 36, no. 4, pp. 38–45, April 1998.

[3] K. Pahlavan, X. Li, and J.-P. Makela, "Indoor geolocation science and technology," IEEE Communication Magazine, vol. 40, pp. 112–118, February 2002.

[4] Y. Zhao, "Standardization of mobile phone positioning for 3G systems," IEEE Communication Magazine, vol. 40, pp. 108–116, July 2002.

[5] J.-C. Chen, C.-S. Maa, and J.-T. Chen, "Factor graphs for mobile position location," in Proc. IEEE International Conference on Acoustics, Speech, and Signal Processing (ICASSP) 2003, vol. 2, April 2003, pp. 393–396.

[6] F. R. Kschischang, B. J. Frey, and H.-A. Loeliger, "Factor graphs and the sum-product algorithm," IEEE Trans. on Information Theory, vol. 47, no. 2, pp. 498–519, February 2001. [7] T. Qiao and H. Liu, "An improved method of moments estimator for toa based localization," IEEE Communications Letters, vol. 17, no. 7, pp. 1321–1324, July 2013.

[8] C. Mensing and S. Plass, "Positioning based on factor graphs," EURASIP Journal on Advances in Signal Processing, vol. 2007, no. ID 41348, pp. 1–11, April 2007.

[9] H. Liu, F. K. W. Chan, and H. C. So, "Non-line-of-sight mobile positioning using factor graphs," IEEE Trans. on Vehicular Technology, vol. 58, no. 9, pp. 5279–5283, November 2009.

[10] J.-C. Chen, Y.-C. Wang, C.-S. Maa, and J.-T. Chen, "Network side mobilepositionlocationusing factorgraphs," IEEE Trans. on Wireless Comm., vol. 5, no. 10, pp. 2696–2704, October 2006.

[11] C.-T. Huang, C.-H. Wu, Y.-N. Lee, and J.-T. Chen, "A novel indoor RSS-based position location algorithm using factor graphs," IEEE Trans. on Wireless Comm., vol. 8, no. 6, pp. 3050–3058, June 2009.

[12] P. Bahl and V. Padmanabhan, "Radar: an in-building rf-based user location and tracking system," in INFOCOM 2000. Nineteenth Annual Joint Conference of the IEEE Computer and Communications Societies. Proceedings. IEEE, vol. 2, 2000, pp. 775–784.

[13] J. C. Wang, L. S. Huang, H. L. Xu, B. Xu, and S. L. Li, "A novel range free localization scheme based on voronoi diagrams in wireless sensor networks," Journal of Computer Research and Development, vol. 45, no. 1, pp. 119–125, 2008.

[14] M. R. K. Aziz, K. Anwar, T. Yamaguchi, S. Arata, and T. Matsumoto, "Monitoring spot configuration of RSS-based factor graph geolocation technique in outdoor WSN environment," in IEICE General Conference 2015, March 2015.

[15] S. Cai, H. Pan, Z. Gao, N. Yao, and Z. Sun, "Research of localization algorithm based on weighted voronoi diagrams for wireless sensor network," EURASIP Journal on Wireless Communications and Networking, vol. 50, pp. 1–5, 2014.

[16] Y. S. Cho, J. Kim, W. Y. Yang, and C.-G. Kang, MIMO-OFDM Wireless Communications with MATLAB. Wiley, 2010.